

# Isothermal and non-isothermal crystallization of PP: effect of annealing and of the addition of HDPE

H. P. Blom<sup>a</sup>, J. W. Teh<sup>b</sup>, T. Bremner<sup>b</sup> and A. Rudin<sup>a,\*</sup>

<sup>a</sup>Department of Chemistry, University of Waterloo, Waterloo, Ontario, Canada N2L 3G1

<sup>b</sup>Novacor Research and Technology Corporation, 2928–16 Street N.E., Calgary, Alberta, Canada T2E 7K7

(Received 15 August 1997; revised 8 November 1997; accepted 12 November 1997)

In this report, we present the results of our investigation into the crystallization behaviour of polypropylene. The crystallization process was followed by hot-stage optical microscopy, differential scanning calorimetry, and dynamic mechanical methods. As well, nuclear magnetic resonance spin–spin relaxation techniques were employed to probe the morphology of the polypropylene. Nucleation in this isotactic polypropylene was athermal and appeared to be heterogeneous. The dependence of the onset temperature of crystallization on the annealing temperature and on the annealing time indicated that PP nuclei were able to survive the melting process. Nuclear magnetic resonance spin–spin relaxation experiments indicated that the PP melt contained a significant proportion of regions of high segment density. It was postulated that these ‘ordered’ regions acted as nucleation sites for PP crystallization, and that the number and size of these regions was determined by the annealing time and temperature. Addition of HDPE to PP resulted in melting-point depression and plasticization of the PP phase at lower HDPE contents. HDPE was able to penetrate the PP phase sufficiently at lower HDPE contents to reduce the number and size of regions of high segment density, thereby delaying the nucleation and subsequent crystallization of the PP phase. © 1998 Elsevier Science Ltd. All rights reserved.

(Keywords: polypropylene, polyethylene, blends; NMR; crystallization)

## INTRODUCTION

In recent years, blends of crystallizable polymers have been receiving increasing attention. In particular, it has been recognized that the properties of these blends are very dependent on the crystallinity, crystalline morphology, and degree of dispersion of the blend<sup>1–4</sup>. These initial observations have led several research groups to investigate more closely the crystallization behaviour of blends of semi-crystalline materials, in particular those in isotactic polypropylene and linear polyethylene<sup>5–10</sup>. However, the results presented in these publications are quite divergent. Wenig and Meyer<sup>5</sup> concluded that the ‘growth of the PP spherulites is not influenced by the presence of the PE domains. The spherulitic growth rates do not vary with the composition.’ This was seen as an indication that the PE is not able to effectively penetrate the PP phase. The unstated implication is that this is further evidence for the immiscibility of PP and PE. Bartczak and co-workers<sup>6–8</sup> found that the number of PP nuclei increased with PE content if crystallization was performed at crystallization temperatures ( $T_c$ ) below 127°C, while the number of nuclei decreased at  $T_c > 127°C$ . This was attributed in part to the migration of heterogeneous nuclei from the PP phase to the PE phase during melt mixing. Wenig and Meyer<sup>5</sup> and Bartczak *et al.*<sup>8</sup> have determined that the presence of PE did not effect the spherulite growth rate, while Kudláček *et al.*<sup>10</sup> found that this growth rate was effected by the presence of PE.

Rybníkář<sup>9</sup> has taken this disagreement as the starting point for his own investigation into the crystallization and morphology in PP/PE blends. Although the focus of this author was largely on the effect of PP phase, it was also reported that PE had no effect on the rate or character of PP crystallization.

The most common methods for following the crystallization behaviour of polymers are hot-stage optical microscopy, dilatometry, and differential scanning calorimetry (DSC)<sup>11–13</sup>. Hot-stage optical microscopy can be used to determine the spherulite growth rate as well as the nucleation density. Dilatometry follows the change in density of the sample, and DSC is used to determine the enthalpy of fusion, and the melting or crystallization temperature of the material. Recently, a report<sup>14</sup> has appeared outlining the use of dynamic mechanical methods to follow the crystallization process. Typically, a PP melt will have a modulus on the order of  $10^3$  Pa, while the modulus of the solid is  $\sim 10^8$  Pa. The dynamic mechanical method assumes that during crystallization, the nuclei that form will act like physical cross-links. These cross-links will increase the modulus of the material. As crystallization proceeds, the nuclei develop into spherulites. This resembles a composite, with the spherulites as hard spheres and the remaining melt as the matrix. The authors postulated that the initial increase in modulus was thus due to the nucleation of the blend, and that any further increase was due to spherulitic growth. Using this technique, it was possible to follow the nucleation and crystallization of PP and PP/high-density polyethylene (HDPE) blends.

\* To whom correspondence should be addressed

The one element about which there is full agreement between the various research groups that have studied PP crystallization is that the addition of PE resulted in a decrease in the number of PP nuclei. The agreement stops there, however. As has already been pointed out, Bartczak and co-workers<sup>8</sup> argued that the PP nuclei migrated to the PP phase. Rybníkář<sup>9</sup> found this explanation unconvincing. Clearly, there is room for more investigation in this area. What is the fate of the nuclei in the PP phase?

Nuclear magnetic resonance (NMR) spin relaxation methods are becoming more accepted as a means of probing the morphological characteristics of polymers. Bremner and Rudin<sup>15</sup> have recently published the results of their  $T_2$  (spin-spin or transverse relaxation) investigation of polyethylene melts. Some of the relevant considerations of that report will be presented here. The reader is referred to reference 15 for further details and references.

Since the  $T_2$  relaxation is sensitive to translational and diffusional processes of molecules, it can be used to delve into the morphology of a polymeric material. In general, a densely packed material will have a shorter relaxation time than a material that is less densely packed. The authors give as an example a semicrystalline polymer which comprises amorphous and crystalline domains. The crystalline domains will have a shorter  $T_2$  than the amorphous domains, since the crystalline domains have a higher segment density than the amorphous regions. It is also possible to determine the component contributions to the total signal, and thereby the relative fractions of each material can be determined. Although the above approach is somewhat artificial in that it limits the number of discrete phases, it has been used by several researchers.

The experiment involves the determination of a  $T_2$  relaxation curve. In the above report this curve was then fitted to the sum of three exponentials, from which the relaxation times and fractions for the three components could be obtained. A two component fit and a four component fit were also attempted, but were rejected because of a poor fit and duplicate  $T_2$ 's, respectively. The authors assumed that the material consisted of three components, (i) non-network amorphous material, (ii) entangled network material, and (iii) ordered material in the melt. The fraction of the 'ordered' component from the NMR analysis correlated very well with the degree of crystallinity from DSC. This was taken as evidence that the HDPE had regions of 'order' or high segment density in the melt.

In this present study, hot-stage optical microscopy, DSC, dynamic mechanical methods, and  $T_2$ -relaxation measurements were used to probe the crystallization behaviour of PP, as well as the effect of HDPE on the crystallization of PP.

## EXPERIMENTAL

### Materials

The PP used in this study was an injection-moulding grade isotactic polypropylene supplied by Shell Canada Limited. It had a melt flow index (MFI) of 20 dg min<sup>-1</sup> (230°C, 2.16 kg). The molecular weight as determined by size exclusion chromatography<sup>16</sup> was  $M_n = 21\,700$ ,  $M_w = 166\,000$ , and  $M_z = 509\,000$  ( $M_w/M_n = 7.6$ ). The polypropylene had a density of 0.91 g cm<sup>-3</sup>. High density polyethylene was supplied by DuPont Canada Inc., and had an MFI of 5 dg min<sup>-1</sup> (190°C, 2.16 kg). It had a density

of 0.96 g cm<sup>-3</sup>, and a molecular weight of  $M_n = 16\,000$ ,  $M_w = 72\,600$ , and  $M_z = 256\,000$  ( $M_w/M_n = 4.5$ ).

### Sample preparation

The PP/HDPE blends (100/0 to 0/100 PP/HDPE by 10% increments) were dry blended prior to melt-blending on an injection molder (Battenfeld BSKM 50-ton press) at the following conditions: 190–210°C barrel temperature, 3.22 MPa injection pressure, 40°C mold temperature, and 1.2 second injection time. The injection molded impact bars, tensile bars, and runners were ground on a Wiley mill. This procedure of melt-blending followed by grinding was repeated once more. The neat homopolymers were also subjected to the above treatment.

For the NMR investigation, a plaque (10x10x12 cm) was compression molded at 200°C, after which it was cooled slowly (~30°C/hour) in the hot-press.

### Optical microscopy

Two microscope slides (20x50x0.16 mm) were placed on a hot-plate set at 210°C underneath a metal weight (0.65 kg). After thermal equilibrium had been reached, a small pellet (~10 mg) of polymer was introduced between the two slides, and the weight returned. At the same time, the temperature on a Reichert hot-stage optical microscope was set to the desired crystallization temperature (131, 134, or 137°C). The polymer was kept on the hotplate for 15 minutes, after which it was rapidly transferred with tweezers to the hot-stage microscope. Thermal equilibrium at the crystallization temperature was achieved in a short time (<60 s) due to the small mass of the slides and polymer. Timing of the crystallization process began as soon as the polymer was transferred to the microscope. The spherulite diameter was monitored by means of a vernier inscribed in the eyepiece of the microscope. Also, the number of spherulites within the field of view in the eyepiece were counted to obtain an estimate of the average nucleation density. Reported results for spherulite growth rate and nucleation density were averages of at least three measurements.

### Differential scanning calorimetry (DSC)

A Perkin Elmer DSC-2 was used to monitor the crystallization behaviour of the homopolymers and blends. A polymer sample (~10 mg) was weighed accurately, sealed in an aluminium pan, and placed in the DSC cell which had been set at the starting temperature (170–200°C). The sample reached this starting temperature within one minute of loading. The cell was continuously purged with nitrogen. The sample was held at the starting temperature for a desired time (15 or 25 min), and then cooled at 1.25°C min<sup>-1</sup> to 100°C. The peak crystallization temperature, onset temperature, and the heat of fusion were calculated by the supplied software.

### Dynamic mechanical analysis

Pellets (~1 g) of PP and PP/HDPE blends were introduced between the 25 mm-diameter parallel plates of a Rheometrics 605 dynamic mechanical spectrometer, and pressed into a disk of 2 mm thickness at the desired starting temperature (170, 180, or 200°C). The heating time was held constant at either 15, 25, or 45 minutes. Dynamic mechanical measurements were carried out using a low strain of 0.8% at a frequency of 1 rad s<sup>-1</sup>. These values were chosen to ensure that the dynamic shearing would not disturb the crystallization process, and to ensure that the

measurement could be carried out to the largest extent of crystallization before the torque on the transducer reached its limiting load. In the case of isothermal crystallization, the polymer was cooled from the starting temperature to the desired crystallization temperature (131, 134, or 137°C) at  $10^{\circ}\text{C min}^{-1}$ . Due to the large mass of the sample and sample enclosure, a step change in temperature could not be achieved. Some overshoot in temperature was unavoidable. In the case of non-isothermal crystallization, the polymer was cooled from the starting temperature at  $1^{\circ}\text{C min}^{-1}$  until the torque reached the limit of the transducer. Data analysis, method, and interpretation of results are described in further detail in reference 14.

#### Nuclear magnetic resonance spin-spin relaxation experiments

The samples were used as prepared, and placed in 5 mm diameter NMR tubes prior to evacuation under a vacuum of  $5 \times 10^{-4}$  mm Hg for a period of 48 hours.

The proton NMR  $T_2$  relaxation times were measured on a Bruker AC-300 NMR spectrometer operating at a proton frequency of 300.13 Hz. This non-solids spectrometer was modified in such a way as to allow external digitizer address advance sampling of single data points in the tops of each of the spin echoes which produces the  $T_2$  decay directly. A water-cooled 5 mm dual probe ( $^1\text{H}/^{13}\text{C}$ ) was used for all experiments, with temperature stability of  $\pm 0.1^{\circ}\text{C}$ . Typical  $90^{\circ}$  pulse times of 9.5 microseconds were obtained, and probe dead times of 15 microseconds were found to be adequate to prevent pulse breakthrough. The standard CPMG pulse sequence was used<sup>17,18</sup> with careful attention to phase cycling to avoid spin-locking at short inter-pulse ( $\tau$ ) spacings<sup>19</sup>. For all samples, 4000 data points were taken to define the decay, ensuring a good baseline. The  $180^{\circ}$

interpulse spacing in all cases was held constant at 50 microseconds, as variation of this time has been shown to alter the time constants of decay in heterogeneous systems<sup>20</sup> such as those under study here. A more detailed description of the NMR experiment, including a discussion of the parameters and setup, are given in Ref. 15. A discussion of the errors in this experimental method is also provided in Appendix I of Ref. 15.

## RESULTS AND DISCUSSION

### Crystallization behaviour of *i*-PP

A typical plot for the increase in spherulite diameter with time as monitored by optical microscopy is shown in Figure 1. It is clear that the radial growth rate remained constant with time in the case of isothermal crystallization. In several cases, crystallization was allowed to continue until spherulite impingement occurred, after which the sample was melted at  $190^{\circ}\text{C}$  for 10 minutes, and then cooled to the crystallization temperature. It was found that the nucleation occurred at the same position and spherulites reformed in the same place. This indicates either that the nucleation was heterogeneous, or that the nuclei were not destroyed completely at  $190^{\circ}\text{C}$  for 10 minutes. Further, it was noted that nucleation was essentially athermal, as evidenced by its time-independence. Athermal, heterogeneous nucleation of *i*-PP has been reported by others<sup>8,13</sup>.

Figure 2 outlines the effect of crystallization temperature ( $T_c$ ) on the spherulite radial growth rate and on the nucleation density. As pointed out in Section 2, each data point is an average of 3–5 replicates. Only one point in Figure 2 has error bars because the agreement for the other points was excellent. The nucleation density was

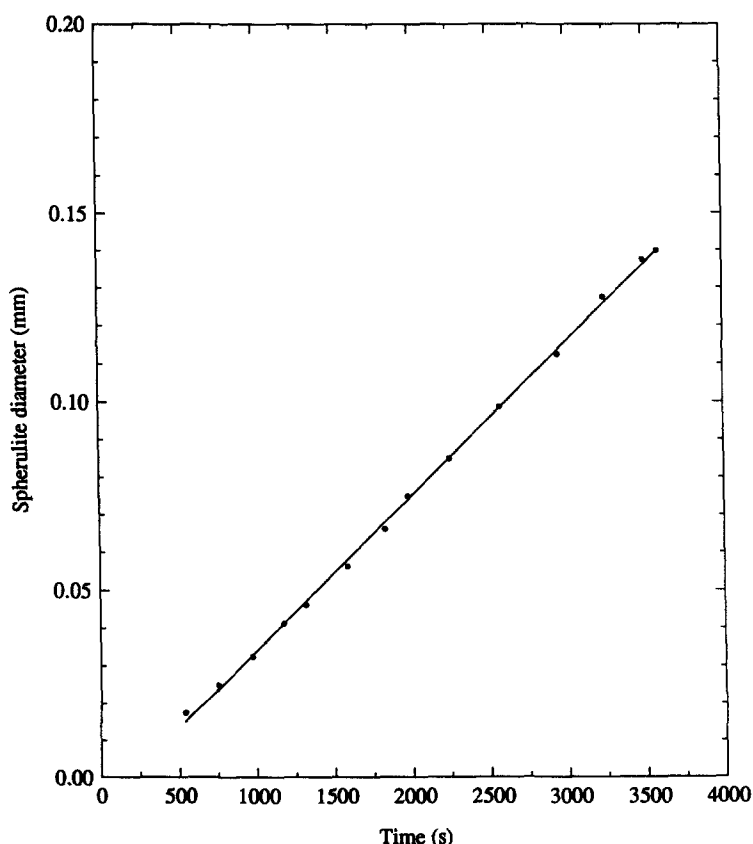
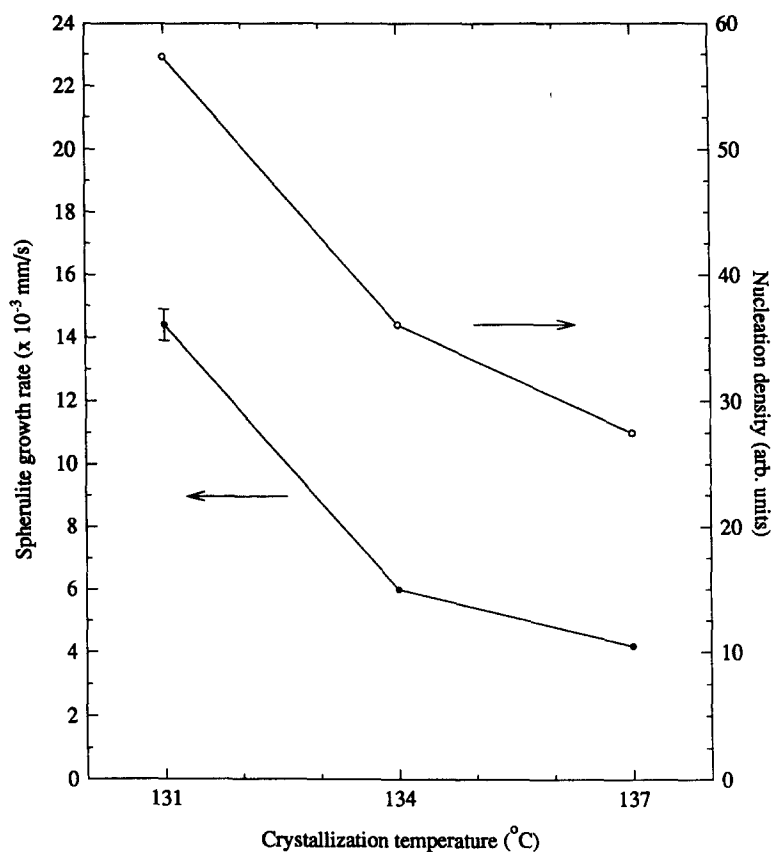


Figure 1 Typical growth profile of a PP spherulite as monitored by optical microscopy.  $T_c = 137^{\circ}\text{C}$ , slope = radial growth rate =  $4.1 \times 10^{-5}$  mm s



**Figure 2** Variation of growth rate of PP spherulites and nucleation density as a function of crystallization temperature, as monitored by optical microscopy

determined from the optical microscope study by counting the number of spherulites that could be observed in the eyepiece at the end of the experiment. Since the visible area remained constant for each experiment, as did the thickness of the film ( $\sim 70 \mu\text{m}$ ), the number of spherulites can be taken as an indication of the nucleation density of the sample. It is clear from *Figure 2* that both the spherulite radial growth rate and the nucleation density decreased as  $T_c$  increased. The growth rate is faster the higher the degree of undercooling of the melt (or the lower the crystallization temperature), as a result of the nucleation-controlled character of crystal growth<sup>13</sup>. The observation that the nucleation density decreased with increasing  $T_c$  suggests that fewer active nuclei exist at higher temperatures. An active nucleus is one that is of a critical size such that it is stable, and persists, permitting further growth. This observation indicates that nucleation is dependent on temperature, and hence heterogeneous nucleation is ruled out.

The results of the DSC investigation of *i*-PP crystallization are shown in *Figure 3*. PP was crystallized from 170°C, 180°C, and 200°C at a cooling rate of  $1.25^\circ\text{C min}^{-1}$ . From the DSC melting curve of PP at a heating rate of  $5^\circ\text{C min}^{-1}$  it was found that the final melting temperature ( $T_m$ ) of the PP was 167°C. Thus, the samples which were melted and annealed at 170°C were only slightly above  $T_m$ , and these samples would be more susceptible to minor variations in thermal history or processing than the samples which were melted and annealed at 180°C and 200°C.

*Figure 3b* (180°C holding temperature) shows that as the annealing time was increased,  $T_{\text{onset}}$  decreased slightly ( $\sim 1^\circ\text{C}$ ). This was also true in the case of the 200°C holding temperature, but was not observed for the 170°C holding temperature (*Figure 3a*). In this case,  $T_{\text{onset}}$  actually

increased slightly with increasing time. In the case of annealing at 170°C the spread of data for duplicate runs was of the order of  $\pm 1^\circ\text{C}$ , whereas in the case of 180°C and 200°C, the reproducibility was within  $\pm 0.2^\circ\text{C}$ .

From *Figure 3c* (constant annealing time  $t = 15$  min) it can be seen that as the annealing temperature was increased,  $T_{\text{onset}}$  decreased ( $T_{\text{onset}} = 132, 129,$  and  $127^\circ\text{C}$  at holding temperatures of 170, 180, and 200°C, respectively). Not only was  $T_{\text{onset}}$  affected by the holding temperature, but also the peak width, the peak height, and the peak crystallization temperature were affected. As the annealing temperature was increased, the peak height increased and the peak width at half-height decreased. It should be noted that the heat of fusion (which is determined from the peak area, and is thus related to the peak height and width) was independent of annealing times and temperatures, and remained essentially constant for all samples, within experimental error. This indicates that complete melting of the major crystalline phase has taken place for the melting and annealing conditions used. However, crystallites or nuclei may have been destroyed to different extents, leading to a different kinetics and rate of crystallization as reflected by the different  $T_{\text{onset}}$  and peak temperatures as well as the width at half height.

The variation of  $T_{\text{onset}}$  with annealing temperature as determined from these DSC experiments was quite small. When dynamic mechanical methods are used to monitor the non-isothermal crystallization of PP, similar trends are observed, but with greater differences. In these experiments, the sudden change in slope that occurs as the sample is cooled can be taken as an indication of the onset of nucleation (although it may coincide with crystallization), as has been described in a recent publication by Teh *et al.*<sup>14</sup>. It is clear from *Figure 4a* that, as suggested earlier, if PP is

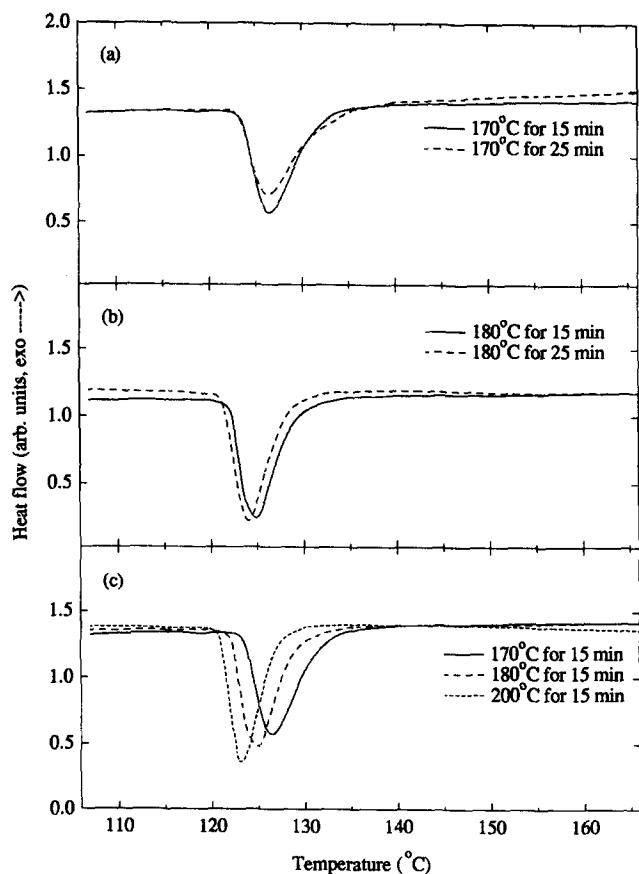


**Figure 3** DSC traces for PP, displaying the effect of annealing temperature and annealing time

annealed at 170°C prior to crystallization, the data are not very reproducible. In fact, the range of  $T_{\text{onset}}$  determined for several samples under identical conditions is  $\sim 5^\circ\text{C}$ . However, in the case of annealing at 180°C, the reproducibility is very good ( $\sim 0.5^\circ\text{C}$ ), as can be seen in Figure 4b. The observed variation in  $G'$  in the liquid region before nucleation began is likely due to experimental errors such as the presence of trapped air bubbles or excess material around the edge of the parallel plates of the instrument. The differences are small, and are considered to be insignificant.

Figure 4c outlines the change in storage modulus ( $G'$ ) with temperature during the non-isothermal ( $1^\circ\text{C min}^{-1}$ ) crystallization of *i*-PP from 170°C and from 180°C. We can see from these experiments that as the melting and annealing temperature was increased, the onset of nucleation was delayed to a lower temperature (from  $\sim 147^\circ\text{C}$  to  $\sim 128^\circ\text{C}$  in this case). Or put differently, the degree of supercooling increased as the annealing temperature increased. This further supports the postulation of incomplete destruction of nucleating crystallites at 170°C as discussed previously.

The result of our investigation into the morphology of *i*-PP by nuclear magnetic resonance spin-spin relaxation experiments at various temperatures is shown in Figure 5. This data represents the results of a three component fit of the  $T_2$  relaxation curve. The solid lines represent the normalized component intensities and the dashed lines the  $T_2$ 's. Thus, each component is defined by an intensity and a relaxation time. The  $T_2$  relaxation times increased as the temperature increased, as expected due to the thermal expansion of the matrix. The relative amount of the component with the longest  $T_2$  changed very little as the

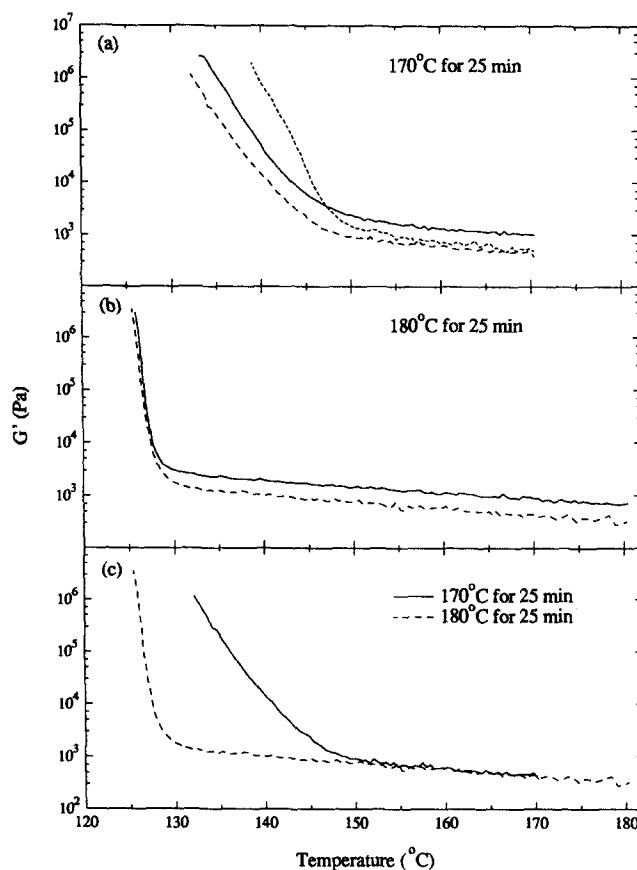


**Figure 4** Effect of the annealing temperature on the crystallization behaviour of PP, as monitored by the dynamic mechanical test

temperature increased from 70°C to 190°C. The contribution of the component with an intermediate  $T_2$  remained constant ( $\sim 31\%$ ) until the temperature reached 120°C, after which it increased to 55% at 190°C. The fraction of the material with the shortest  $T_2$  decreased gradually from 70°C to 140°C (68% to 48%), after which it decreased drastically. At 190°C, this component accounted for  $\sim 25\%$  of the signal. The  $T_2$  relaxation time for this component remained nearly constant between 70°C and 120°C, after which it increased rapidly.

As has been stated in the introduction, we know that the material with the highest segment density will have the shortest  $T_2$  (i.e. relax the fastest), while the material with the lowest segment density will have the longest  $T_2$  (i.e. relax the slowest). We also know from DSC measurements (heating at  $5^\circ\text{C min}^{-1}$ ) that the PP used in this investigation had a melting temperature of 167°C (range from  $\sim 140^\circ\text{C}$  to 167°C). The degree of crystallinity of this PP<sup>21</sup> (from DSC) is 55–60%. And finally, we know that PP is a semicrystalline material, a property it shares with high density polyethylene.

Following the example set by Bremner and Rudin, let us tentatively assign the fastest relaxing (shortest  $T_2$ ) component to the ordered crystalline region of the sample, the slowest relaxing (longest  $T_2$ ) component to the unentangled amorphous region, and the intermediate component to the entangled network region. This means, therefore, that at 70°C, the degree of crystallinity of the sample is  $\sim 68\%$ . This is high when compared to the result in reference 21. However, the present sample was slow cooled in the hot-press, and therefore a higher degree of crystallinity would be expected. The degree of crystallinity decreased steadily as

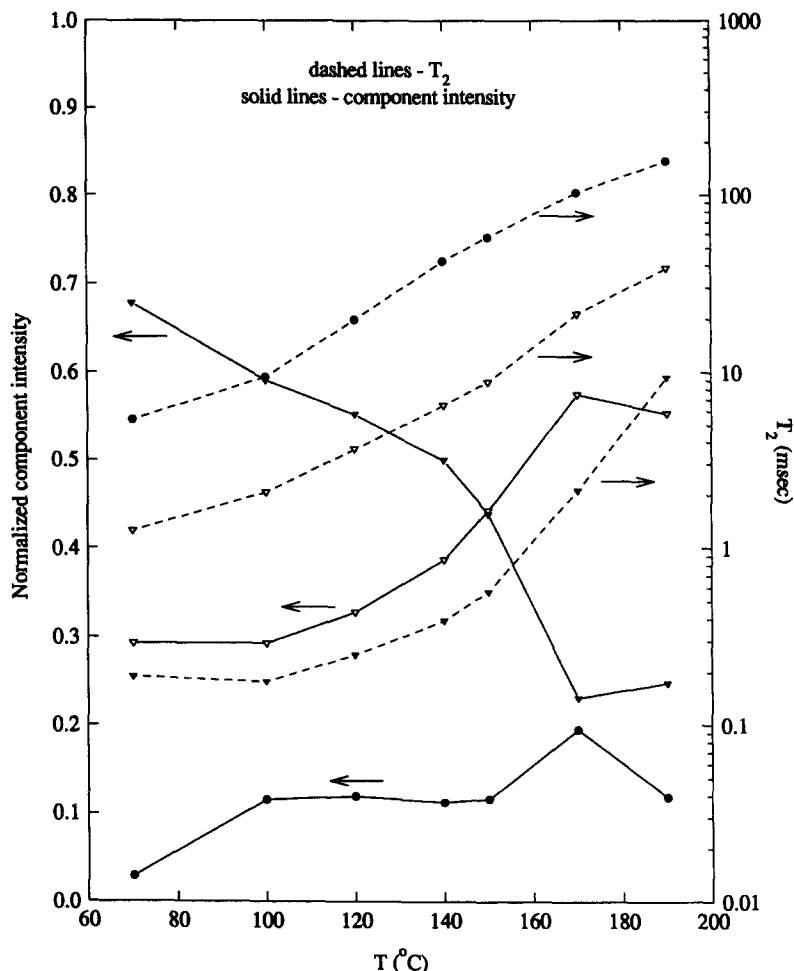


Figure 5 The temperature dependence of the relaxation times and component intensities for PP, based on a three component fit of the  $T_2$  relaxation curves

the temperature was increased. As the temperature rose above 140°C, the degree of crystallinity decreased more rapidly until 170°C, after which it levelled off at about 25%. This agrees well with the melting temperature range as determined from DSC. The contribution to the total  $T_2$  signal from the intermediate component behaved in an opposite fashion to the crystalline component. Whereas the amount of crystalline material decreased as the temperature was increased, the amount of entangled network material increased as the temperature increased. The amount of amorphous material remained constant with temperature. This suggests that melting involved a mass transfer from the crystalline phase to the entangled phase, which is expected.

If we consider the above analysis of the NMR data as plausible, then we must also conclude that the PP melt includes some 'quasi-indestructible clusters'<sup>22</sup>, and has regions of high segment density. In fact, the component intensity of the 'ordered' (pseudo-crystalline) region at 190°C is approximately 25%. In other words, ~25% of the PP melt is in an 'ordered' state. Although surprising, this is not completely unexpected, considering that similar results have been observed for HDPE. Also, molecular dynamics simulations of PP chains in vacuum indicate the presence of helical segments at 500 K<sup>23</sup>.

In 1950, D. Turnbull<sup>24</sup> published a paper on the kinetics of heterogeneous nucleation. In this report, he attempted to explain the observed effect of thermal history on the kinetics of liquid–solid transformations. It had been observed in many cases of bulk crystallization that a certain amount of

super-cooling,  $\Delta T_-$ , was required before crystallization would occur. Further, it was found that the amount of super-cooling required was related to  $\Delta T_+$ , the difference between  $T_m$  and the temperature to which the material was taken above  $T_m$ . The relation is shown schematically in Figure 6. As  $\Delta T_+$  increased,  $\Delta T_-$  increased rapidly at first, and then became essentially independent of  $\Delta T_+$ . This data suggested that destruction of nuclei took place at a temperature higher than that of  $T_m$ , and that some nuclei were able to survive the melting process, and that the number of these nuclei decreased as  $\Delta T_+$  increased. At some value of  $\Delta T_+$ , all the nuclei were destroyed, and the  $\Delta T_-$  became independent of  $\Delta T_+$ . Earlier, Richards and co-workers<sup>25,26</sup> had proposed that extraneous structures (i.e., adventitious impurities) could retain crystallite adsorbates above  $T_m$ . As the temperature increased above  $T_m$ , these adsorbed crystallites became less stable, and eventually disappeared. Turnbull<sup>24</sup> developed this work further, and showed mathematically that crystallites could indeed be stabilized in conical and cylindrical cavities.

Recently, a variation of this theory was invoked by Rybníkář<sup>9</sup> to explain the observed stabilization of polyethylene nuclei above the  $T_m$  of the PE in PP/PE blends. It was suggested that when PP/PE blends were annealed at temperatures above  $T_m$ (PE) and below  $T_m$ (PP), that PE nuclei and/or crystallites were stabilized in the PP matrix. Subsequent cooling to the crystallization temperature resulted in the expulsion of the PE crystallites from the PP matrix as a result of stresses in the PP matrix.

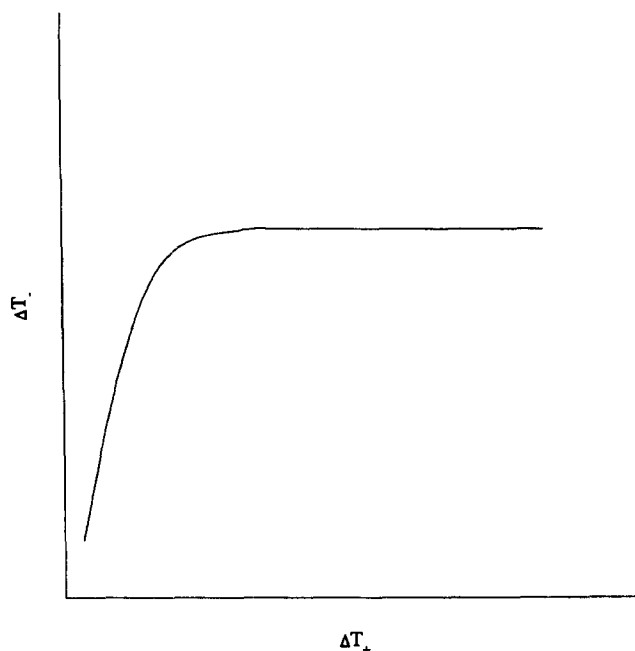


**Figure 6** Schematic diagram of the effect of heating above  $T_m(\Delta T_+)$  on the supercooling ( $\Delta T_-$ ) necessary to achieve nucleation in a given time

That PP crystallites or nuclei might be absorbed into cracks and crevices of adventitious impurities can not be denied. Certainly, the proposal of Turnbull has merit. However, our NMR data indicates that the PP melt at 190°C is heterogeneous, and that a significant proportion (as much as 25%) of the PP melt at 190°C is in a loosely ordered state. Clearly, not all of this material can be said to reside in or on extraneous structures. Therefore, although Turnbull's hypothesis might serve to explain the presence of some persistent nuclei, it cannot account for the stability of the majority of the quasi-crystalline material in the PP melt.

It is clear from our crystallization study (DSC and DMA) that we have also observed a dependence of  $T_{\text{onset}}$  (which is related to  $\Delta T_-$ ) on the degree of heating above  $T_m(\Delta T_+)$ , although in our case we do not seem to have come to the plateau where  $\Delta T_-$  becomes independent of  $\Delta T_+$ . From the foregoing discussion, it seems reasonable to suggest that, in this situation, the behaviour observed in *Figure 6* is a consequence of the persistence of regions of high segment density above the  $T_m$  of PP. At 170°C, there are a great many of these clusters, since the annealing temperature is only slightly above  $T_m$ . As the annealing temperature increased (annealing time remained constant), these clusters became more loosely bound or the number of clusters decreased. As the annealing time increased (constant annealing temperature), the size and/or number of these clusters diminished, as indicated by the decreased in  $T_{\text{onset}}$ , since crystal growth can only occur when the nuclei have reached a critical size. At sufficiently high temperatures, an equilibrium number and size of these quasi-crystalline clusters is reached, and  $\Delta T_-$  becomes independent of  $\Delta T_+$ .

Nucleation of this type has been termed self-nucleation or self-seeding<sup>13</sup>. In this case, crystal growth occurs on remnants of crystals that survived the melting step.  $\Delta T_-$  is seen to vary with  $\Delta T_+$  as previously described in *Figure 6*. In all cases, self-nucleation is heterogeneous and athermal. Clearly, our data are very much in line with this type of nucleation. The NMR experiments performed in this investigation indicate that the nuclei that survive melting

are not necessarily stabilized in adventitious cracks but rather that the PP melt is non-homogeneous. 'Ordered' regions persist in the melt, and the characteristics of this 'order' are determined by the thermal history of the material, and this 'order' in turn affects the crystallization behaviour of the PP.

All of this, of course, does not preclude the existence of other nucleating centres such as calcium stearate or impurities. However, it would not be expected that these nuclei would display a temperature dependence as has been observed. Further, the effect of these nuclei is assumed to be constant. Therefore, while the presence of other nucleating centers is highly probable, we are concerned at present only with those nuclei that display a dependence on annealing time and annealing temperature.

### CRYSTALLIZATION OF PP/HDPE BLENDS

The effect of high-density polyethylene on the crystallization behaviour of polypropylene as determined by optical microscopy is shown in *Figures 7* and *8*. In *Figure 7*, the change in spherulite radial growth rate with HDPE content at different crystallization temperatures is plotted, and in *Figure 8* the variation of nucleation density with HDPE content at  $T_c = 134^\circ\text{C}$  is plotted (the results at 131°C and 137°C are similar). It is apparent that while the spherulite growth rate remained essentially unchanged as the HDPE content was increased, the nucleation density decreased upon addition of 10% HDPE, and then increased gradually with increasing HDPE content. Visually, it was possible to detect and observe the dispersed HDPE droplets when they were encountered by the growing PP spherulite front. They were engulfed by the growing spherulites. No

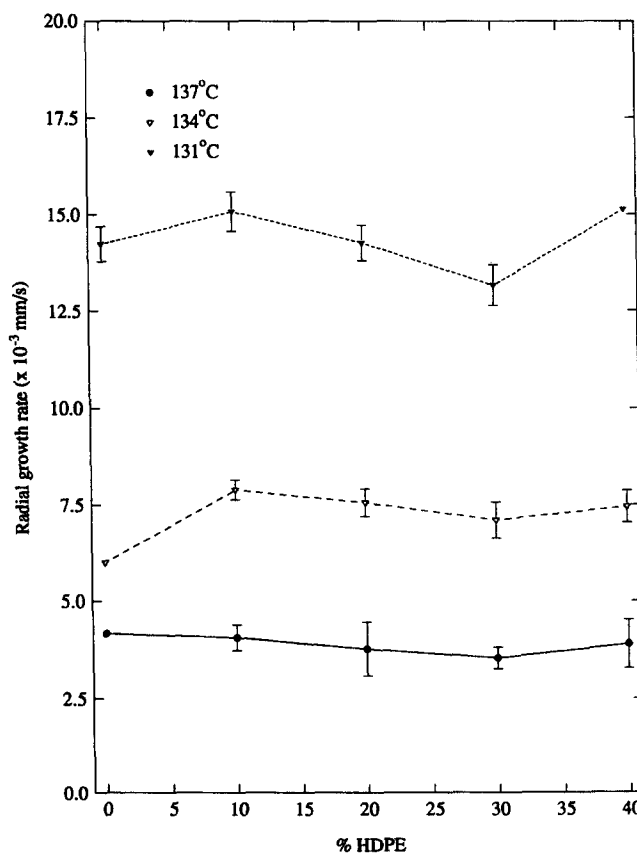


**Figure 7** Dependence of the growth rate of PP spherulites on HDPE content, at three crystallization temperatures (131°C, 134°C, and 137°C)

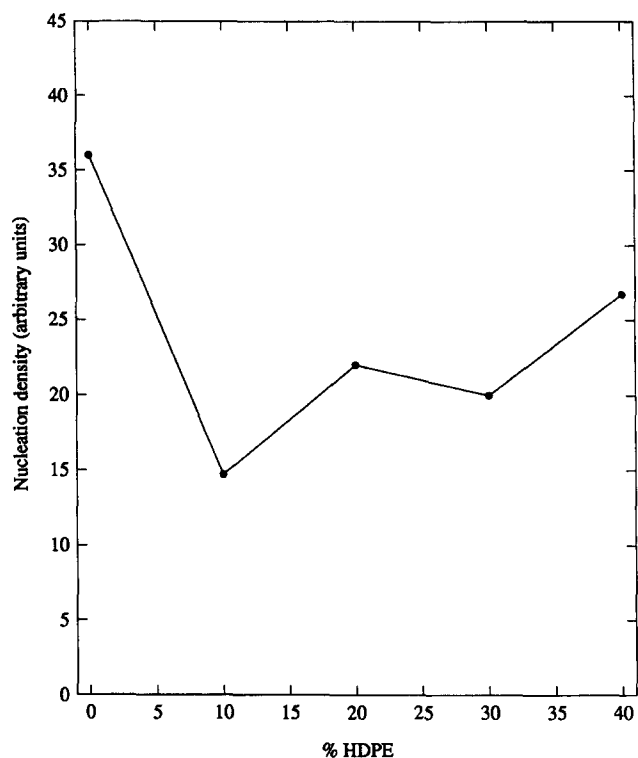


Figure 8 Variation of nucleation density of PP with HDPE content, as monitored by optical microscopy

evidence for droplet deformation was observed, nor were the HDPE droplets pushed along by the spherulite front before engulfment. As the HDPE content was increased, the HDPE droplets increased in size and number, and at 40% HDPE content, a co-continuous morphology was observed. No data were obtained beyond 40% HDPE due to the fact that crystallization was not observed within the time frame of the experiments.

These results agree well with those published by Wenig *et al.*<sup>5</sup>, Bartczak *et al.*<sup>8</sup>, and by Rybníkář<sup>9</sup>. Wenig and

Meyer<sup>5</sup> investigated the crystallization behaviour of PP-PE blends by optical microscopy, and found that the dispersed PE phase had no effect on the PP spherulites. They suggested that this resulted from the immiscibility of the two materials, and that only a very small fraction of the polyethylene penetrated the PP phase.

Bartczak, Galeski, and Pracella<sup>8</sup> studied the crystallization behaviour of PP in the presence of HDPE, and found that the spherulite growth rate remained unchanged over the composition range (0–50% HDPE) studied. However, they noticed that at  $T_c \leq 127^\circ\text{C}$ , the nucleation density increased with HDPE content, but that at  $T_c > 127^\circ\text{C}$ , the nucleation density decreased with HDPE content. These authors concluded that heterogeneous nuclei were migrating from the PP phase to the HDPE phase during the melt-mixing process. The driving force was said to arise from interfacial energy differences. Thus, at  $T_c > 127$  above the nucleation temperature of HDPE, as the HDPE content was increased, the number of PP nuclei was seen to decrease. At  $T_c \leq 127^\circ\text{C}$ , the crystallites of HDPE which can form at this lower temperature act as nucleation sites for the PP, and thereby increase the nucleation density of the PP, even though more heterogeneous nuclei would have migrated from the PP phase with increasing HDPE content.

Rybníkář<sup>9</sup> also investigated the crystallization of blends of *i*-PP and HDPE. Although the primary focus of this investigation was the effect of PP on the crystallization behaviour of HDPE, this author also found that the presence of PE had no influence on the PP crystallization.

DSC crystallization curves (non-isothermal, constant cooling rate =  $1.25^\circ\text{C min}^{-1}$ ) for PP and PP/HDPE blends (100/0 to 60/40 PP/HDPE) are shown in Figure 9. There are a number of interesting observations to be made from this figure. It is apparent that for the 90/10 PP/HDPE blend, a single crystallization peak was observed, indicating that the PP and the HDPE crystallized at the same time. Also, this blend has an onset temperature which is about  $2.5^\circ\text{C}$  lower than that of neat PP. This indicates that for this system the onset of crystallization of PP was delayed. The DSC curve

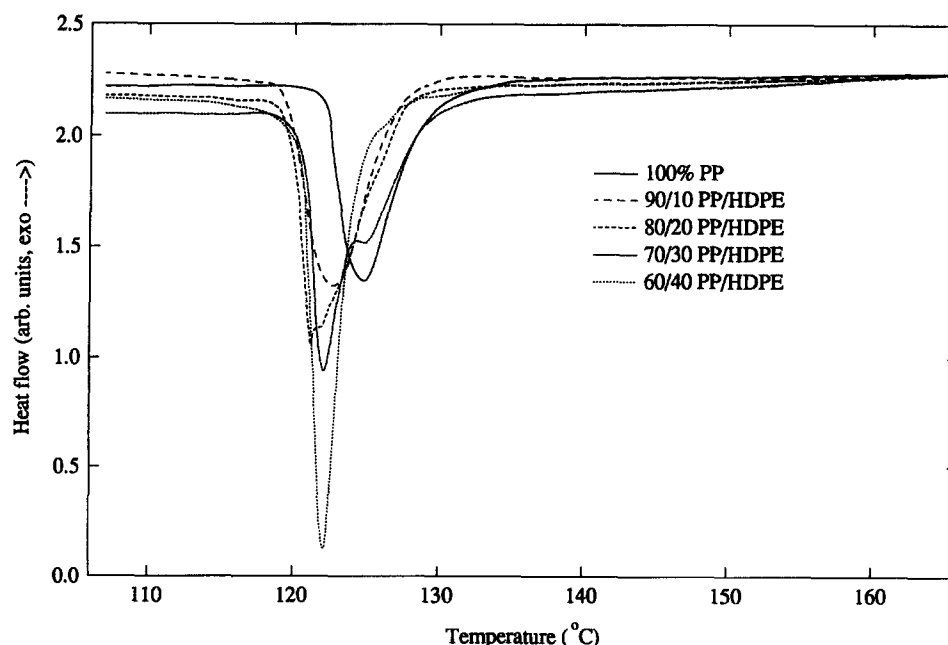


Figure 9 DSC thermograms (crystallization at  $1.25^\circ\text{C min}^{-1}$  cooling rate) of PP and PP-rich PP/HDPE blends



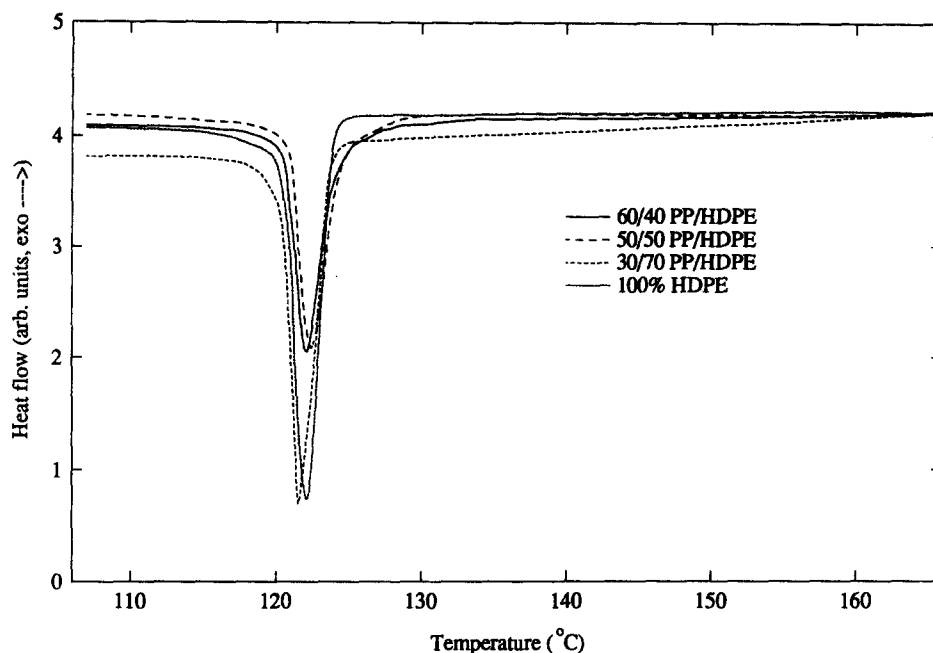


Figure 10 DSC thermograms (crystallization at  $1.25^{\circ}\text{C min}^{-1}$  cooling rate) of HDPE and HDPE-rich PP/HDPE blends

for the crystallization of the 80/20 PP/HDPE blend showed a broad crystallization endotherm with two poorly resolved peaks, with an onset temperature similar to the 90/10 PP/HDPE blend. The 70/30 PP/HDPE blend clearly shows a main peak closer to that of HDPE, with a distinct shoulder at a higher temperature closer to the crystallization peak of PP. The shoulder is the PP peak and the main peak is due to the HDPE. (Note: HDPE has a much larger heat of fusion than *i*-PP. Therefore, although HDPE is the minor component in the 70/30 blend, it will produce a larger peak in the DSC.) For this sample, it is difficult to determine the onset temperature due to the limitations of the Perkin Elmer software. Addition of a further 10% HDPE (60/40 PP/HDPE blend) again resulted in a single higher temperature peak on the DSC, and it was no longer possible to distinguish between crystallization of the PP and that of the HDPE.

The DSC traces of the HDPE-rich PP/HDPE rich blends (60/40 to 0/100 PP/HDPE) are shown in Figure 10. It is clear that there is essentially no change in  $T_{\text{onset}}$  for these samples. The only evidence for the presence of PP in these blends can be found in the shapes of the curves. Neat HDPE had a sharp onset temperature, while the 60/40 and 50/50 PP/HDPE blends displayed a gradual onset.

Figure 11 summarizes the onset temperatures for all the samples investigated by DSC as a function of PP content. Even though the 80/20 and 70/30 PP/HDPE data may not be completely reliable (*viz.* Figure 9), it is clear that as the PP content decreased to the 70% level,  $T_{\text{onset}}$  decreased steadily. Further addition of HDPE had no effect on  $T_{\text{onset}}$ .

Investigation of the non-isothermal crystallization of PP/HDPE blends by dynamic mechanical analysis yielded the results shown in Figure 12. It should be noted that duplicate runs on different days indicate a reproducibility in the onset temperature of  $\sim 0.5^{\circ}\text{C}$ . Thus, a difference in onset temperature of  $1^{\circ}\text{C}$  is certainly significant. It is clear from Figure 12 that the onset of nucleation for the neat PP and the neat HDPE are distinct. In the case of the blends, the onset temperature decreased as HDPE was added to the PP. It is interesting to note that the 30/70 PP/HDPE blend had a lower onset temperature ( $\sim 1^{\circ}\text{C}$ ) than neat HDPE, as did the

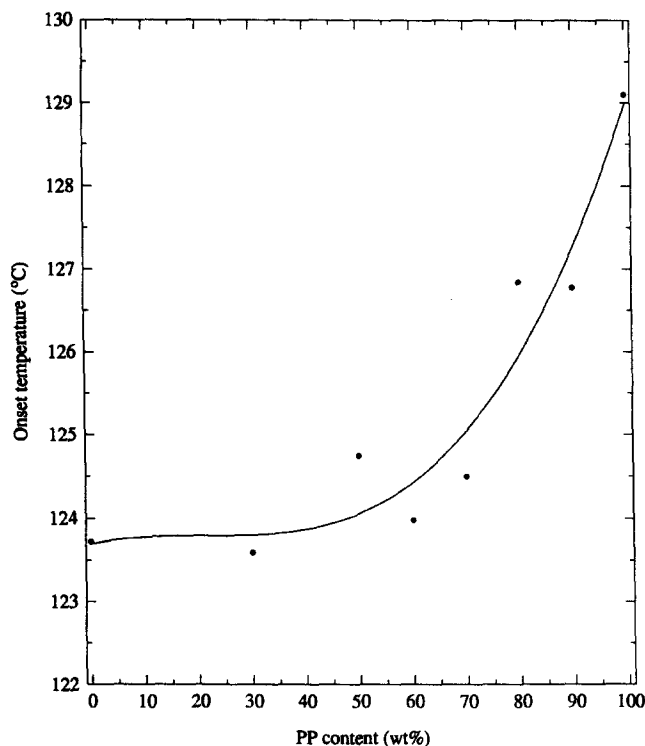


Figure 11 Variation of  $T_{\text{onset}}$  with PP content, as determined from DSC analysis

10/90 PP/HDPE blend (this curve lay between those for the 30/70 PP/HDPE blend and the neat HDPE, but is not shown for reasons of clarity). This figure also indicates a difference in the storage modulus of the melt before nucleation and crystallization commenced. As the HDPE content increased in the blends,  $G'$  decreased steadily. One should not place too much importance on this observation, however. It was noted from the duplicate experiments that there existed some variability in this melt regime, as discussed previously. These slight variations in the sample did not effect the onset temperature.

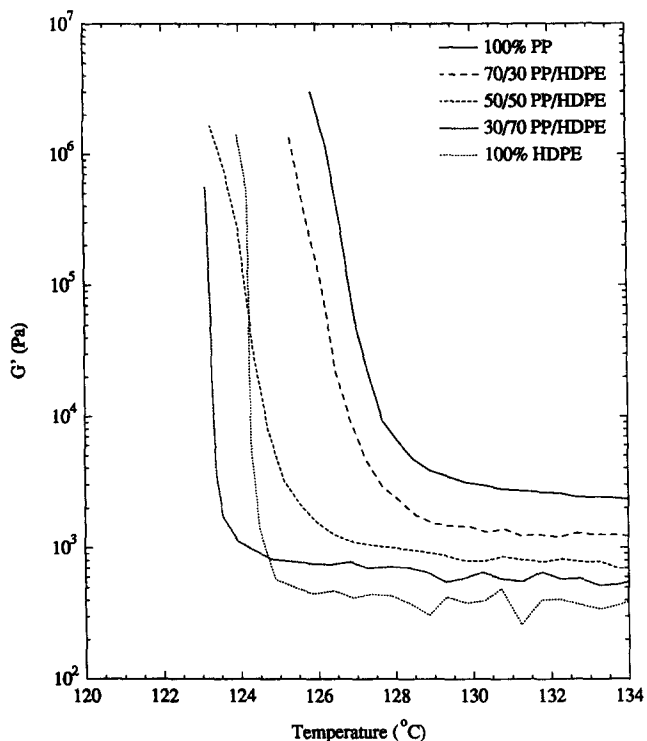


Figure 12 Variation of  $T_{onset}$  for PP, PP/HDPE blends, and HDPE, as determined from the dynamic mechanical analysis under non-isothermal cooling conditions

Figure 13 outlines the results of the isothermal crystallization ( $T_c = 137^\circ\text{C}$ ) of PP and PP/HDPE blends. The first point to note is that the temperature profile during the experiment indicates that the sample temperature dropped to well below the crystallization temperature. This is, however, somewhat misleading. The thermocouple measured the temperature of the upper plate in contact with the melt, not the actual sample temperature. As polymers are poor conductors of heat, it is reasonable to expect that the temperature of the sample will lag behind during a step

change in temperature. That the sample temperature is not truly indicated by the first part of the temperature profile (time  $< 1000$  s) can also be seen by the modulus trace in that region. The modulus would have exhibited a slight maximum where the sample temperature was a minimum, followed by a slight decrease as the sample warmed up again to  $T_c$  if the temperature of the sample had the same profile. This was not seen. It can be safely concluded, therefore, that the sample temperature did not dip appreciably below  $T_c$ .

The results plotted in Figure 13 are quite complex, and it is difficult to explain the full modulus curve completely at this time. All the curves increased initially at essentially the same rate due to the sudden drop in temperature of the system indicating a change in the melt modulus with temperature. This was followed by a period of constant modulus, the duration being dependent on the sample. At some point, the modulus began to increase steadily from  $10^3$  to  $10^6$  Pa after which the curves were seen to level off. For HDPE contents greater than 70%, no nucleation and crystallization were observed at  $137^\circ\text{C}$  up to 8250 s.

In an earlier report<sup>14</sup> slightly different curves were obtained, in that the final part of the curve was also linear on a semi-log plot. The first region was attributed to nucleation, and the latter to growth. The present data differs in that the high- $G'$  region was not linear on a semi-log plot. However, this present study differed slightly from the previous one in that here the samples were held at  $180^\circ\text{C}$  prior to crystallization, and in the former study the samples were annealed at  $170^\circ\text{C}$ . As we have already seen, the annealing temperature has a significant impact on the crystallization behaviour of PP. Under the conditions used in the present investigation, more nuclei were destroyed as a result of the higher melting and annealing temperature, and hence the curves obtained (c.f. Figure 13) show that nucleation and growth were occurring together.

There are two main results that should be stressed from this isothermal crystallization study. The first is that addition of 10% HDPE delayed the nucleation of PP (90/10 PP/HDPE blend). Addition of 30% HDPE also

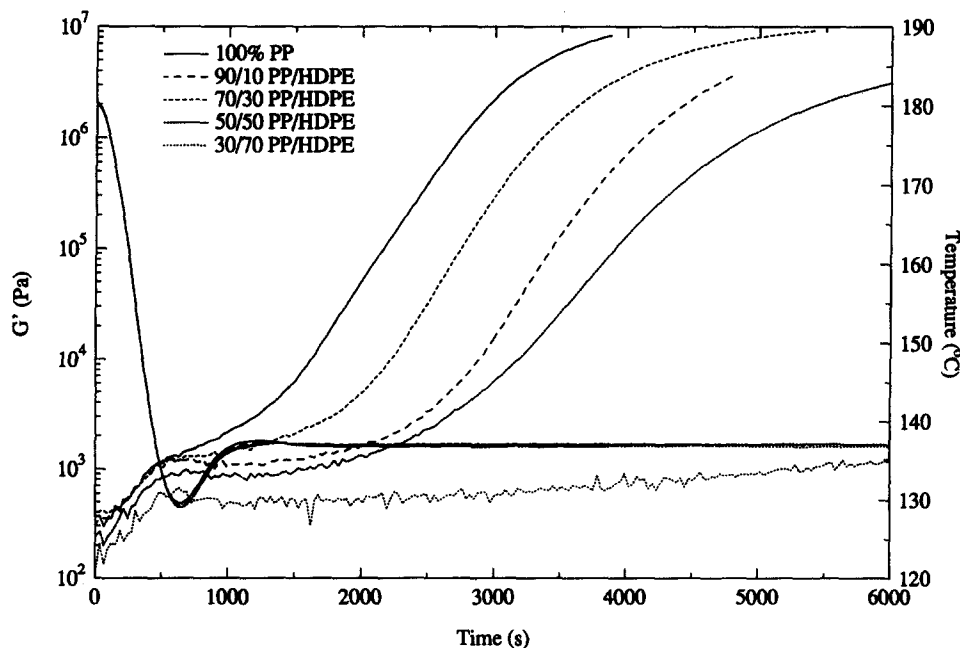


Figure 13 Effect of composition on the isothermal crystallization behaviour of PP/HDPE blends at  $T_c = 137^\circ\text{C}$  obtained by dynamic mechanical tests

delayed the nucleation of PP, but to a much lesser extent than 10% HDPE. The 50/50 PP/HDPE blend had a  $G'$ -profile similar to the 90/10 blend. The second important observation is that the slopes of the  $G'$  curves after nucleation had begun is the same for samples for which the HDPE content was less than or equal to 30%.

Summarizing the results thus far, we have seen from the isothermal crystallization study on the optical microscope that the spherulite growth rate of PP was not affected by addition of HDPE to PP, but that the nucleation density decreased by ~50% upon addition of 10% HDPE to PP. HDPE droplets were engulfed by the PP spherulites. From the DSC investigation (non-isothermal crystallization), it was found that addition of HDPE to PP resulted in a decrease in the onset temperature for crystallization up to 40% HDPE. Further addition of HDPE had no effect on  $T_{\text{onset}}$ . Dynamic mechanical analysis (DMA) was also used to study the isothermal and non-isothermal crystallization behaviour of PP. From both experiments it was found that HDPE delayed the onset on nucleation of the PP melt. These results indicate that HDPE had an effect on the crystallization behaviour of PP. What remains is to determine the nature of this effect.

We saw in the previous section that the PP melt had regions of high segment density. It was argued that these "ordered" regions acted as the nuclei in the crystallization of PP, and that the number and size of these nuclei was determined by the thermal history of the sample. As the annealing temperature was increased, the size of these nuclei was reduced, and the effect of this was to delay the onset of crystallization. In the present case, we have also observed a decrease in  $T_{\text{onset}}$ , except that now the variable is the HDPE content. This suggests that HDPE is in some way reducing the size and/or number of nuclei (polymer aggregates) in the PP. In other words, HDPE may be acting as a diluent or plasticizer for PP. This is consistent with Doolittle's 'gel theory'<sup>27</sup> of plasticization, which states that two equilibria operate simultaneously in a plasticized material. One is the solvation-desolvation equilibrium between solvent and solute, and the other is the aggregation-disaggregation equilibrium between solute molecules. The net effect is that the solvent serves to oppose (and reduce) the aggregation of the polymer molecules. The solvating strength of a diluent is related to its solubility in the polymeric material, and thus is a function of the miscibility of the solvent and the solute.

The variation of  $T_{\text{onset}}$  with HDPE content is reminiscent of melting point depression phenomena. It is well-known that the melting point of a crystallizable polymeric material can be reduced by addition of a diluent. This has been observed in cases where the diluent is a small molecule, but it has also been observed in the case where the diluent is a macromolecule. Nishi and Wang<sup>28</sup> studied the crystallization behaviour of a poly(vinylidene fluoride)-poly(methyl methacrylate) (PVF<sub>2</sub>-PMMA) blend. It was found that PMMA depressed the melting point of the PVF<sub>2</sub>, and this melting point depression could be explained in terms of the thermodynamic mixing of a crystalline polymer and an amorphous material. These authors derived an analytical expression for the melting point depression observed in this system, equation (1),

$$\frac{1}{T_m} - \frac{1}{T_m^0} = - \frac{RV_{2u}}{\Delta H_{2u}V_{1u}} \chi_{12}(1 - v_2)^2 \quad (1)$$

where the subscripts 1 and 2 refer to the macromolecular diluent and the crystallizing polymer, respectively,  $T_m$  is the

measured melting point,  $T_m^0$  is the melting point of the pure material,  $v$  is the volume fraction,  $V$  is the repeating unit molar volume,  $\Delta H_{2u}$  is the repeating unit molar heat of fusion, and  $\chi_{12}$  is the diluent-polymer interaction parameter. The important point to note in the above equation is that  $\chi_{12}$  must be negative for melting point depression to occur. Further,  $\chi_{12}$  will only be negative if the polymer and the diluent are miscible, which was the case for PVF<sub>2</sub> and PMMA.

The implication of the above consideration is that PP and HDPE exhibit some miscibility under the conditions of these experiments. Therefore, our investigation indicates that the PP and HDPE used in this investigation are partially miscible at lower HDPE contents (this is where the greatest reduction in  $T_{\text{onset}}$  was observed) when melt-blended on an injection molder. There is perhaps only a small degree of intermixing on the molecular level, but it is sufficient to cause observable melting-point depression and plasticization.

## CONCLUSIONS

It has been shown that nucleation in this isotactic polypropylene is athermal and appeared to be heterogeneous. The dependence of the onset temperature of crystallization on the temperature to which the sample was heated above the melting temperature and on the duration of that annealing treatment indicated that PP nuclei were able to survive the melting process. Nuclear magnetic resonance spin-spin relaxation experiments indicated that the PP melt was heterogeneous, and that the PP melt contained a significant proportion of regions of high segment density. It was postulated that these "ordered" regions acted as nucleation sites for PP crystallization, and that the number and size of these regions was determined by the annealing time and temperature.

Addition of high density polyethylene to polypropylene had the same effect on the onset temperature of crystallization as did the annealing temperature and time. It was found that addition of HDPE to PP resulted in melting-point depression and plasticization of the PP phase at lower HDPE contents. HDPE was able to penetrate the PP phase sufficiently at lower HDPE contents to reduce the number and size of regions of high segment density, thereby delaying the nucleation and subsequent crystallization of the PP phase.

## ACKNOWLEDGEMENTS

The authors gratefully acknowledge the financial support of the Natural Sciences and Engineering Research Council of Canada, the University Research Incentive Fund of Ontario, and Montell Canada Limited.

## REFERENCES

1. Martuscelli, E., Pracella, M., Avella, M., Greco, R. and Ragosta, G., *Makromol. Chem.*, 1980, **181**, 957.
2. Gupta, A. K., Gupta, V. B., Peters, R. H., Harland, W. G. and Berry, J. P., *J. Appl. Polym. Sci.*, 1982, **27**, 4669.
3. Teh, J. W., *J. Appl. Polym. Sci.*, 1983, **28**, 605.
4. Lovinger, A. J. and Williams, M. L., *J. Appl. Polym. Sci.*, 1980, **25**, 1703.
5. Wenig, W. and Meyer, K., *Colloid & Polymer Sci.*, 1980, **258**, 1009.
6. Bartczak, Z., Galeski, A. and Martuscelli, E., *Polym. Eng. Sci.*, 1984, **24**, 1155.

7. Bartczak, Z., Galeski, A., Martuscelli, E. and Janik, H., *Polymer*, 1985, **26**, 1843.
8. Bartczak, Z., Galeski, A. and Pracella, M., *Polymer*, 1986, **27**, 537.
9. Rybníkář, F., *J. Macromol. Sci.-Phys.*, 1988, **B27**, 125.
10. Kudláček, L., Kaplanová, M. and Knape, F., *Faserforsch. Textiltech.*, 1978, **29**, 286.
11. Sharples, A., *Introduction to Polymer Crystallization*. Edward Arnold, London, 1966.
12. Mandelkern, L., *Crystallization of Polymers*. McGraw-Hill, New York, 1964.
13. Wunderlich, B., *Crystal Nucleation, Growth, Annealing, in Macromolecular Physics*, Vol.2. Academic Press, New York, 1976.
14. Teh, J. W., Blom, H. P. and Rudin, A., *Polymer*, 1994, **35**, 1680.
15. Bremner, T. and Rudin, A., *J. Polym. Sci., Polym. Phys.*, 1992, **30**, 1247.
16. Pang, S., and Rudin, A., in *ACS Symposium Series 521, Chromatography of Polymers: Characterization by SEC and FFF*, ed. Th. Provder. American Chemical Society, Washington, D. C., 1993.
17. Carr, H. Y. and Purcell, E. M., *Phys. Rev.*, 1954, **94**, 630.
18. Meiboom, S. and Gill, D., *Rev. Sci. Instr.*, 1958, **29**, 688.
19. Suh, B. J., Borsa, F. and Torgenson, D. R., *J. Mag. Res., Series A*, 1994, **110**, 58.
20. Whittaker, A. K., Bremner, T. and Zelaya, F., *Polymer*, 1995, **36**, 2159.
21. Blom, H. P., Teh, J. W. and Rudin, A., *J. Appl. Polym. Sci.*, 1996, **60**, 1405.
22. Rabesiaka, J. and Kovacs, A. J., *J. Appl. Phys.*, 1961, **32**, 2314.
23. Choi, P., Blom, H., Kavassalis, T. A. and Rudin, A., *Macromolecules*, 1995, **28**, 8247.
24. Turnbull, D., *J. Chem. Phys.*, 1950, **18**, 198.
25. Richards, W. T., *J. Appl. Chem. Soc.*, 1932, **54**, 479.
26. Richards, W. T., Kirkpatrick, E. C. and Hutz, C. E., *J. Appl. Chem. Soc.*, 1936, **58**, 2243.
27. Ritchie, P. D. (ed.) *Plasticisers, Stabilisers, and Fillers*. Iliffe Books Ltd., London, 1972, p. 44.
28. Nishi, T. and Wang, T. T., *Macromolecules*, 1975, **8**, 909.